

Apparent T^2 dependence of the normal-state resistivities and lattice heat capacities of high- T_c superconductors*

G. W. Webb, Z. Fisk, and J. J. Engelhardt

Institute for Pure and Applied Physical Sciences, University of California, San Diego, La Jolla, California 92093

S. D. Bader

Argonne National Laboratory, Argonne, Illinois 60439

(Received 8 March 1976; revised manuscript received 17 September 1976)

We report new measurements of the normal-state electrical resistances of several high- T_c (~ 20 K) A-15 structure superconductors. It is found that the resistances are linear functions of T^2 from T_c to 40 K. Analysis of available lattice heat-capacity data on the same materials shows that it also varies as T^2 over the same temperature interval. These observations suggest that the T^2 resistivity is due to electron-phonon scattering. This interpretation is supported by the results of a model calculation for the temperature dependence of the resistivity and the lattice-heat capacity of Nb_3Sn .

I. INTRODUCTION

The class of intermetallic compounds having the A-15 structure is of much interest because it contains materials with the highest superconducting transition temperature (T_c). The high T_c materials have been found to have unusual normal-state properties,¹ many of which are not well understood. Among these is the normal-state electrical resistivity. Woodward and Cody² first called attention to the anomalous electrical resistivity (ρ) in Nb_3Sn , a high- T_c A-15 compound. They found empirically that

$$\rho = \rho_0 + \rho_1 T + \rho_2 e^{-T_0/T}, \quad (1)$$

where ρ_0 , ρ_1 , ρ_2 are constants independent of temperature T , and $T_0 = 85$ K fits their data closely from $T = 18$ to 800 K. Several theoretical models were considered by them in order to explain Eq. (1) but none was found to be satisfactory. Later it was noted³ that the low-temperature resistivity of Nb_3Sn can be fit rather well to a simpler T^2 law but over the smaller temperature range from T_c to 50 K. Similarly, the low-temperature resistivity of the isostructural high- T_c compound V_3Si was found to follow a T^2 law,⁴ and also a better fit to Eq. (1) over a wider temperature range.⁵

As the resistivities of the high- T_c A-15 structure materials are anomalous over the whole range of measurement temperatures, it is not surprising that a variety of physical ideas have been employed in trying to understand them. At the highest measurement temperatures, ≥ 1000 K, the resistivity shows strong negative curvature. At these temperatures the magnitude of the resistivity has risen to above $100 \mu\Omega \text{ cm}$, and appears to be saturating at a value corresponding to an electron mean free path of order one interatomic spacing.⁶ Over an

intermediate temperature interval, 50–300 K, the resistivity also shows negative curvature. To account for this, two different treatments of electron-phonon scattering have been invoked. The first is based on a model electronic density of states containing sharp structure near the Fermi energy which gives rapid Fermi-level motion with temperatures of order 100 K.⁷ The second treatment focuses attention on the anharmonic hardening of phonon modes with increasing temperature which has been observed by neutron-diffraction experiments on some of these materials.⁸ Both of these models provide an explanation for the observed negative curvature.

Below 50 K the effect of Fermi-level motion is expected to be minimal, based on the deduced Fermi temperatures.⁷ Available neutron-scattering data suggest that phonon mode shifting has largely been arrested,⁹ ruling out anharmonic effects. Thus, below 50 K, we do not expect that the resistivity will be influenced by either of these effects, or by the effect of the conduction-electron mean free path approaching a lower bound. However, we have found that the high- T_c compounds ($T_c \approx 20$ K) Nb_3Sn , Nb_3Al , and Nb_3Ge all have unusual resistivities which vary closely as T^2 in this temperature range while the isostructural low- T_c compound Nb_3Sb ($T_c \approx 0.2$ K)(Ref. 10) has a resistivity which varies approximately as T^3 .⁶ In this temperature range the nonmagnetic transition elements are found to have resistivities with temperature dependences between T^3 and T^5 . A T^3 dependence follows from the Wilson s - d scattering model and a T^5 dependence from the Bloch-Grüneisen model.¹¹ With both models the Debye approximation is assumed for the phonon spectrum. At the lowest temperatures, ~ 1 to 10 K, some of the nonmagnetic transition elements show a T^2 term

in their resistivities which has been explained on the basis of electron-electron scattering.¹² The magnitude of the T^2 term observed in the high- T_c A-15 materials is two orders of magnitude larger than has been observed in the nonmagnetic transition metals. The question posed by our resistivity measurements is whether the T^2 term in the low-temperature resistivity is due to electron-electron scattering or electron-phonon scattering. We have not been able to reconcile the magnitude of the T^2 with current theory for electron-electron scattering.¹² However, we call attention to the fact that available data for the lattice-heat capacity of the high- T_c compounds under study here show a severe departure from Debye-like behavior. In fact, the high- T_c materials with the anomalous T^2 resistivity have a lattice heat capacity also varying as T^2 . We find that a model calculation, using an approximate phonon density of states derived from tunneling¹³ data, shows that the lattice heat capacity can follow from the model as well as a T^2 resistivity from electron-phonon scattering. The model calculation does not provide a coefficient for the T^2 term in the resistivity nor is the model phonon density of states shown to be unique. The calculations do show how a low-temperature resistivity varying as T^2 can arise from electron-phonon scattering.

II. EXPERIMENTAL

Sample resistance measurements were carried out on small specimens using the four-probe technique. A 220-Hz alternating current of 1 mA or less was used with the sample voltage detected by a lock-in voltmeter. Temperature was measured by calibrated Pt- and Ge-resistance thermometers. The errors in temperature measurement are ± 0.1 K below 20 K and ± 0.2 K above 20 K.

X-ray diffraction was used to characterize specimens. These measurements were carried out on an x-ray diffractometer with a diffracted beam monochromator using Cu radiation. Unless otherwise noted the A-15 lattice-parameter determination is accurate to ± 0.001 Å. The sensitivity for the detection of extraneous phases likely to occur in these systems is between 5 and 10 vol.%. The purity of starting materials was at least 99.7% for Nb and 99.9% or greater for Al, Sb, and Ge.

Nb₃Sn specimens were synthesized by closed-tube vapor transport using iodine as the transporting agent. Growth was carried out from 600 to 1000 °C for several months. X-ray diffraction of the transported deposits showed only the A-15 structure with a lattice parameter of 5.290 Å. In some cases small 3-mm single crystals were found in the deposits. Leads were attached to small crystals of irregular shape by spot welding. The Nb₃Al

specimen was prepared by first arc melting together Nb and Al. The specimen was then equilibrated at 1900 °C for 12 min followed by cooling to below 700 °C in 10 sec. By x-ray diffraction and optical metallography it was found to be single phase with A-15 structure. It was then annealed at 700 °C for 50 h. The final composition was estimated to be Nb_{0.754}Al_{0.246} with a measured A-15 lattice parameter of 5.182 Å. Small bars of rectangular shape were cut from the specimen, the ends plated with a thin nickel layer, and leads soldered to the nickel.

The Nb₃Ge film was prepared by chemical-vapor deposition on a molybdenum substrate at 900 °C. By x-ray diffraction the material appeared to be greater than 90% A-15 phase, with a lattice parameter of 5.139 Å measured before grinding, and an average lattice parameter of 5.144 ± 0.002 Å after grinding to -400 mesh powder. For the resistance measurement, a piece of irregular shape was flaked from the substrate. Four leads were then attached to the flake with conducting silver paint.

Nb₃Sb specimens were prepared by closed-tube transport as described previously. For resistivity measurements, four leads were spot welded to long thin bars spark cut from single-crystal deposits.

III. RESULTS

Resistance data for Nb₃Sn are shown in Fig. 1. These data have been normalized such that $R = 1$ at 300 K. The break in slope of the resistance at 51 K is in the range where Nb₃Sn is known to (sometimes) undergo a cubic to tetragonal lattice transformation. The observed resistance ratio, $R(300 \text{ K})/R(T_c) = 12.3$, is apparently somewhat larger

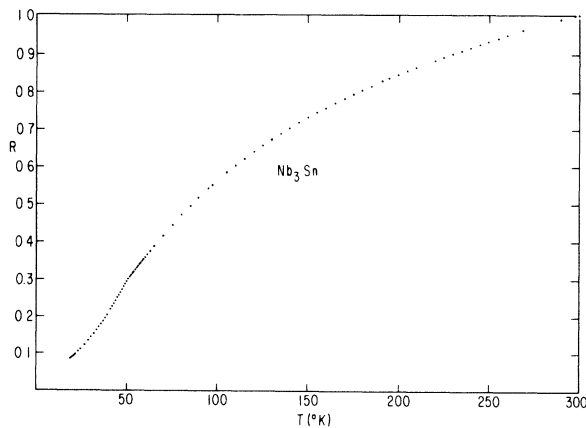


FIG. 1. Resistance of Nb₃Sn from T_c (18.2 K) to 300 K in units where $R(300 \text{ K}) = 1.0$. The kink at 51 K is indicative of a martensitic transformation. Using the data of Woodward and Cody we estimate $\rho(300 \text{ K}) = 75 \mu\Omega \text{ cm}$.

than any other in the literature. The absolute value of the resistivity was not determined because of the specimen's irregular shape. However, an approximate value of $75 \mu\Omega \text{ cm}$ at 300 K was estimated using the data of Woodward and Cody,² with a small correction for different resistance ratios.

Figure 2 shows resistance data for Nb_3Al and Nb_3Ge plotted such that $R=1$ at 300 K. The room-temperature resistivity of the Nb_3Al was found to be $90 \pm 20 \mu\Omega \text{ cm}$. Because of its irregular shape an absolute value for Nb_3Ge was not determined. Others have reported room-temperature values of $80 \mu\Omega \text{ cm}$ for Nb_3Ge specimens with similar resistance ratios.¹⁴ We did not discover any features in the resistance which would suggest a lattice-transformation as is found in Nb_3Sn .

Resistance data for Nb_3Sb are shown in Fig. 3. The room-temperature resistivity is $72 \mu\Omega \text{ cm}$, close to that of Nb_3Sn . No indication for a lattice transformation was found in the resistivity of Nb_3Sb .

In Fig. 4 the low-temperature resistances of Fig. 1 and 2 are shown plotted versus T^2 . As is evident the resistances follow a relation $R=A+BT^2$ rather well from T_c to 40 K. It was not possible to fit the low-temperature Nb_3Sb resistance data to a simple power-law expression as in Fig. 4.

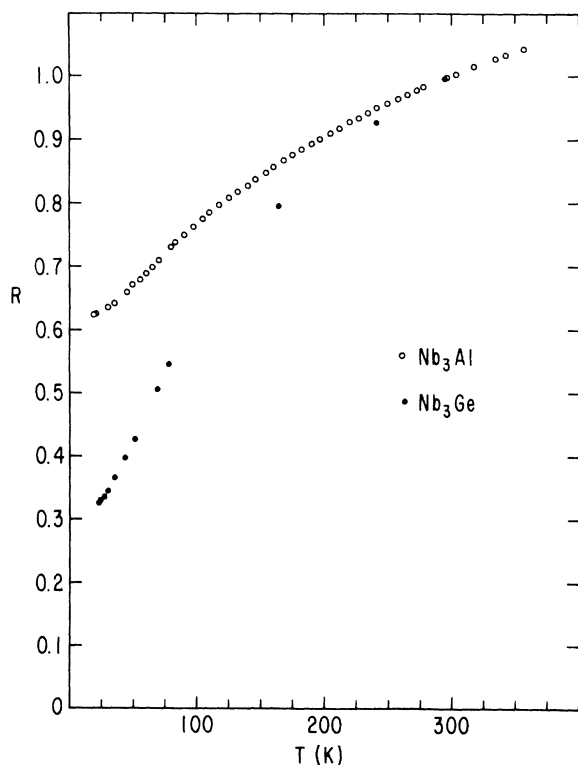


FIG. 2. Resistance vs temperature data for Nb_3Al and Nb_3Ge plotted in units where $\rho(300 \text{ K})=1.0$.

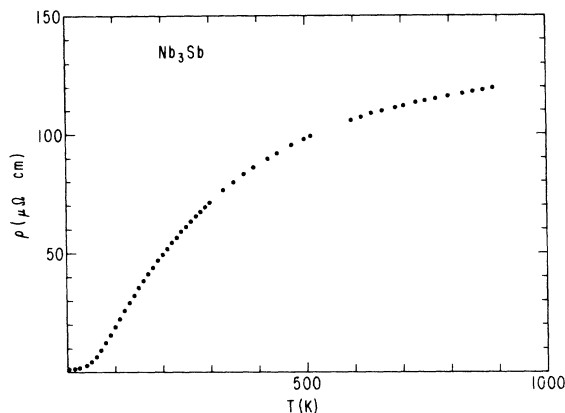


FIG. 3. Resistivity vs temperature data for Nb_3Sb . At 300 K the resistivity is $72 \mu\Omega \text{ cm}$.

Instead the resistance of Nb_3Sb was found to vary approximately as $T^{3.6}$ over the same temperature interval.

IV. DISCUSSION

There are two scattering mechanisms which we expect to be of greatest potential importance in these materials: electron-phonon scattering and

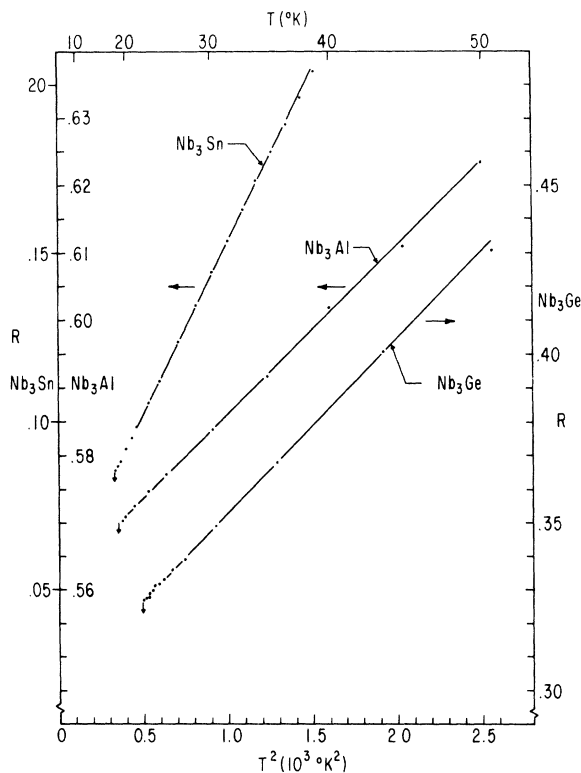


FIG. 4. Low-temperature resistance data for Nb_3Sn , Nb_3Al and Nb_3Ge plotted vs T^2 . The units are such that $\rho(300 \text{ K})=1.0$.

electron-electron scattering. With the assumption of a Debye phonon spectrum having a phonon density of states $f(\omega) \propto \omega^2$, Wilson¹¹ has shown that electron-phonon scattering in transition metals leads to a T^3 dependence to the resistivity at low-temperatures. This is often observed. It has become increasingly evident that the Debye approximation is a poor one for the high- T_c materials under consideration here. These deviations from Debye behavior permit an interpretation of the approximate T^2 dependence to the resistivities in Fig. 4 on the basis of electron-phonon scattering.

A. Resistivity and heat capacity

Figure 5 shows some recent heat capacity¹⁰ data for these materials. Here C_T is the total measured heat capacity. In Figs. 5(a) and 5(b), C_T for Nb_3Sn and Nb_3Al are seen to vary quite closely as T^2 . Near T_c the data were fit¹⁰ to the usual odd-power-of- T series, the first term of which is electronic and the remaining are lattice terms. The additional constraint that the entropies of the superconducting and normal states be equal at T_c was also utilized. This procedure allowed an approximate determination of γ , the enhanced electronic heat-capacity coefficient. The electronic heat capacity has been subtracted from the total measured heat capacity giving the lattice heat capacity C_L shown in Figs. 5(a) and 5(b). The correction for the electronic heat capacity is small, being $\sim 20\%$ at its largest. It is evident that the lattice heat capacity C_L also varies as T^2 and that the inferred temperature dependence is not sensitive to the choice of γ . Figure 5(c) shows that the Debye model for the lattice heat capacity of Nb_3Sb is a good approximation over this temperature range. The electronic heat capacity in Nb_3Sb is not observable on this scale. The γ value for Nb_3Sb is about an order of magnitude smaller than in Nb_3Sn and Nb_3Al . The C_L of Nb_3Sn is also shown in Fig. 5(c) in order to compare it with the Debye model fit to the data at 35 K. It is apparent that the Debye approximation is a poor one for Nb_3Sn over this temperature range.

Because some specimens of Nb_3Sn are known to undergo a tetragonal distortion near 50 K some additional comments are called for. The Nb_3Sn specific-heat specimen of Fig. 5 did show signs in its magnetic susceptibility of undergoing a transformation near¹⁵ 50 K but the effect of the transformation on its heat capacity was not observable. In a detailed investigation¹⁶ into the transformation in Nb_3Sn , Vieland and Wicklund found that transforming samples displayed a small step discontinuity in their specific heats. In a comparison between a sample undergoing the tetragonal dis-

ortion at 50 K and a sample which was not observed to transform by x rays, they found that the tetragonal and cubic materials had indistinguishable heat capacities below 43 and above 59 K. Therefore we conclude that the heat-capacity data

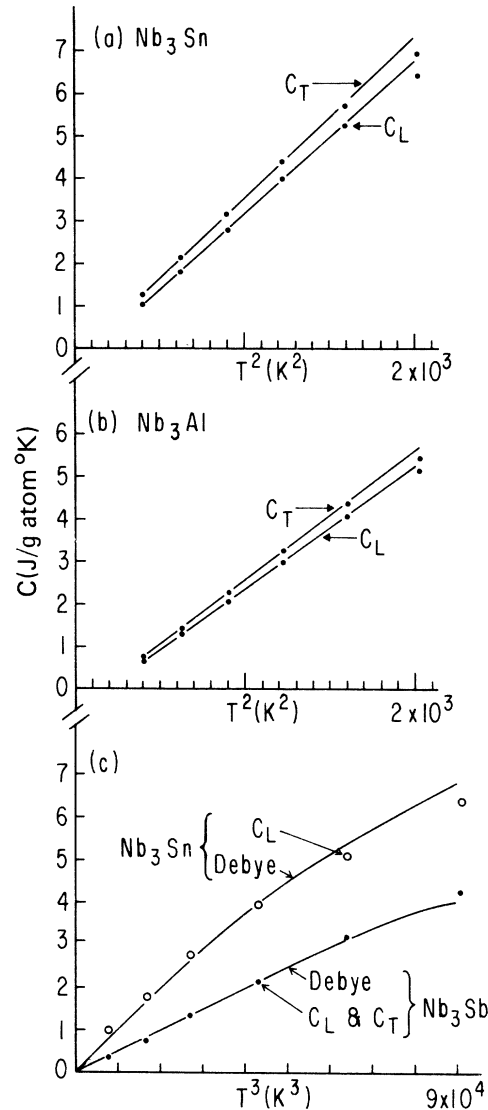


FIG. 5. Shown are heat-capacity vs temperature data taken from Ref. 10. The data extend from 20 to 45 K in 5 K steps. C_T is the total measured heat capacity and $C_L = C_T - \gamma T$ where γ is the electronic capacity coefficient reported in Ref. 10. In (a) and (b), C_T and C_L are seen to vary approximately as T^2 . The negative intercepts in (a) and (b) are a result of T^2 being unphysical as an extrapolation function; at the lowest temperatures C_L must go over to the T^3 dependence of an elastic continuum. In (c) it is evident that the Debye model works well for Nb_3Sb but is a poor approximation for Nb_3Sn over this temperature range. The Debye fits were made at 35 K with $\Theta_D = 336$ and 265 K for Nb_3Sb and Nb_3Sn , respectively.

of Fig. 5 are representative of both transforming and nontransforming material within the precision of the data.

The temperature dependence of the resistivities of Nb₃Sn, Nb₃Al and Nb₃Ge lattice show effects similar to the heat-capacity. In Fig. 4, it is seen that the resistivities increase as approximately T^2 , rather than the T^3 to T^5 dependence usually observed in nonmagnetic materials containing transition elements. The resistivity of Nb₃Sb rises approximately as $T^{3.6}$ suggesting that the Debye model is a better approximation to the phonon spectrum in this material, in agreement with the heat-capacity results of Fig. 5(c).

Taking the heat-capacity and resistivity data together, we advance the following qualitative conclusions: (i) that in the high- T_c compounds the lattice heat capacity rises approximately as T^2 , rather than T^3 , because of a high density of low-lying (in energy) vibrational modes, (ii) these low-lying modes cause the electron phonon contribution to the resistivity to rise with temperature approximately as T^2 , (iii) there is no evidence in the

heat capacity or resistivity of the low- T_c isostructural compound Nb₃Sb of a high density of low-lying lattice modes. In Sec. IV B we give a model calculation for Nb₃Sn which is compatible with these observations.

B. Model calculations

To show that it is plausible that the T^2 resistivity of these high- T_c superconductors is due to electron-phonon scattering, we performed a model calculation for the case of Nb₃Sn using a realistic model phonon spectrum. For phonon-assisted s - d interband scattering, the resistivity depends on the phonon frequencies ω as follows⁸:

$$R \propto \int \frac{X}{[\sinh(X)]^2} F(\omega) d\omega, \quad (2)$$

where $X = \hbar\omega/2k_B T$, $F(\omega)$ is the phonon density of states, and the proportionality factor contains an average transport electron-phonon coupling parameter connecting s and d states, and the s - and d -band densities-of-states at the Fermi energy, which we take as being independent of temperature below ~ 50 K. The lattice heat capacity in the harmonic approximation is

$$\frac{C_L}{3Nk_B} = \int \left(\frac{X}{\sinh(X)} \right)^2 F(\omega) d\omega, \quad (3)$$

where N is Avogadro's number. In the absence of the actual $F(\omega)$ we used Shen's superconductive-tunneling determination¹³ of $\alpha^2 F(\omega)$ for Nb₃Sn as a basis for constructing an approximate but realistic $F(\omega)$. This is a reasonable approach since $F(\omega)$ and $\alpha^2 F(\omega)$ are expected, in general, to contain similar structure. To extract $F(\omega)$ from $\alpha^2 F(\omega)$ we have set $\alpha^2 = 1 - A\omega$ with $A = 0.033$ (meV)⁻¹. This value of A was chosen so that the model $F(\omega)$ [see inset (a) of Fig. 6] yielded the same geometric mean phonon frequency

$$\omega_g = \left(\prod_{s=1}^{3N} \omega_s \right)^{1/3N} = \exp \left(\int (\ln \omega) F(\omega) d\omega \right) \quad (4)$$

as obtained calorimetrically: $\hbar\omega_g/k_B = 201$ K.¹⁰ $F(\omega)$ is normalized to the correct number of modes. This form for α^2 has the physical significance of attenuating the coupling to higher-frequency phonons, optical modes in the case of Nb₃Sn. The model $F(\omega)$ describes the lattice heat capacity over an appreciable temperature range [see inset (b) of Fig. 6]. The deviation between the measured (solid curve), and calculated (circles) lattice heat capacities in inset (b) of Fig. 6, noticeable at the higher temperatures, is predominantly due to (i) the limitations of our assumption that the electronic heat capacity needed to obtain C_L from the measured heat capacity is

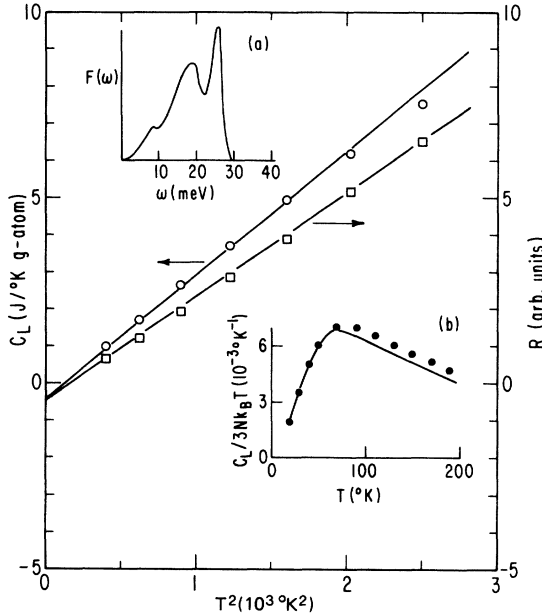


FIG. 6. Calculated resistances (squares, arbitrary units) and lattice heat capacities (circles) for Nb₃Sn plotted vs T^2 between 20 and 50 K. The straight lines (guides for the eye) indicate that the linearity and the negative intercept for C_L observed experimentally are recovered. Inset (a) is the phonon density of states $F(\omega)$ used in the calculation. It has the structure of $\alpha^2 F$ obtained in Shen's tunneling experiment. Inset (b) indicates that the calculated C_L values (circles) are in quite reasonable accord with the measured (Ref. 7) C_L values (displayed as the solid curve) over a large temperature range.

simply γT , and (ii) to the negative nonharmonic contribution to C_L becoming important. Available data show that nonharmonic effects are absent below 50 K.⁹

Figure 6 shows that between 20 and 40 K, the model calculations of C_L and R are linear functions of T^2 , as are the experimental data of Figs. 4 and 5. Outside of this range the model results deviate from a T^2 dependence.

It should be emphasized that the agreement between the experiment and the model calculation shown in Figs. 6 and 6(b) does not provide a very stringent test for the model $F(\omega)$. In fact we have already found another one parameter renormalization of Shen's $\alpha^2 F$ by rescaling the ω axis of $\alpha^2 F$ by the multiplicative factor of 1.23. This rescale factor was chosen so that the new model $F(\omega)$ yielded the same $\omega_c = 201$ K as before. This new $F(\omega)$ gives equally good agreement to the experimental results as that shown in Fig. 6 and 6(b).

The essential difference between the two-model phonon density of states and the Debye phonon density of states commonly used to interpret experimental results is that the models have added strength at low energies, ~ 10 to 20 meV. That the model calculation can only be carried out over a restricted temperature range because of anharmonic effects and because $F(\omega)$ enters the calculation through an integral precludes a more precise treatment. Nevertheless the point is made that electron-phonon scattering can give a qualitative account of the unusual low-temperature resistivity of Nb_3Sn without having to invoke other mechanisms

such as electron-electron scattering.

On the same basis we infer that in Nb_3Al and Nb_3Ge a non-Debye-like phonon density of states is present which is similar to that of Nb_3Sn but which is absent in Nb_3Sb . Indeed, in Nb_3Sb the Debye approximation seems to be quite good in describing the lattice heat capacity. That the resistivity varies as $T^{3.6}$ rather than precisely as the T^3 dependence of the s - d scattering model suggests that the density-of-states is not entirely dominated by the d band. In fact the electronic heat capacity is low, 1.1 mJ/K²g atom,¹⁰ a value typical of non-transition metals. Nevertheless some interband scattering is expected because recent de Haas-van Alphen measurements¹⁷ show that there are at least four sheets to the Fermi surface of Nb_3Sb .

In summary, we find that the isostructural set of high- T_c (~ 20 K) compounds Nb_3Sn , Nb_3Al , and Nb_3Ge exhibit apparent T^2 dependences above T_c to their electrical resistivities and, for Nb_3Sn and Nb_3Al , to their lattice heat capacities. In the case of Nb_3Sn , the existence of tunneling data allow model phonon densities of states to be constructed which reproduces the lattice heat capacity over a decade in temperature, and which explains the unusual electrical resistivity on the basis of electron-phonon scattering without invoking further special features to these materials.

ACKNOWLEDGMENTS

We thank L. J. Sham, G. S. Knapp, F. Y. Fradin, and R. Viswanathan for helpful discussions.

*Research supported in part by the Air Force Office of Scientific Research, Air Force Systems Command, USAF Grant No. AFOSR-74-2664, NSF through Grant No. DMR 75-04019. Work at Argonne National Laboratory supported by the U. S. Energy Research and Development Administration.

¹For a review, see L. R. Testardi, *Phys. Acous.* **10**, 194 (1973).

²D. W. Woodward and G. D. Cody, *Phys. Rev.* **136**, A166 (1964).

³S. J. Williamson (private communication).

⁴V. A. Marchenko, *Sov. Phys.-Solid State* **15**, 1261 (1973).

⁵M. Milewits, H. Taub, and S. J. Williamson, Proceedings of the International Conference on Low Lying Lattice Vibrational Modes and Their Relationship to Superconductivity and Ferroelectricity (unpublished); and Ferroelectricity (to be published).

⁶Z. Fisk and G. W. Webb, *Phys. Rev. Lett.* **36**, 1084 (1976).

⁷R. W. Cohen, G. D. Cohen, and J. J. Halloran, *Phys. Rev. Lett.* **19**, 840 (1967). Also see R. W. Cohen, Conference Proceedings on Superconductivity in d -

and f -Band Metals, Rochester, New York, 1971 (unpublished); and W. Rehwald, M. Rayl, R. W. Cohen, and G. D. Cody, *Phys. Rev. B* **6**, 363 (1972).

⁸P. B. Allen, *Phys. Rev. B* **3**, 305 (1971), especially p. 318.

⁹J. D. Axe and G. Shirane, *Phys. Rev. B* **8**, 1965 (1973).

¹⁰G. S. Knapp, S. D. Bader, and Z. Fisk, *Phys. Rev. B* **13**, 3783 (1976).

¹¹A. H. Wilson, *The Theory of Metals*, 2nd ed. (Cambridge U. P., Cambridge, England, 1956).

¹²M. J. Rice, *Phys. Rev. Lett.* **25**, 1439 (1968).

¹³L. Y. L. Shen, *Phys. Rev. Lett.* **29**, 1082 (1972). α^2 is thought to be dominated by matrix elements connecting d states.

¹⁴H. Leutz, H. Weissmann, O. F. Kammerer, and M. Strongin, *Phys. Rev. Lett.* **36**, 1576 (1976).

¹⁵S. D. Bader, G. S. Knapp, and A. T. Aldred (unpublished).

¹⁶L. J. Vieland and A. Wicklund, *Solid State Commun.* **7**, 37 (1969).

¹⁷A. Arko and Z. Fisk, *Bull. Am. Phys. Soc.* (to be published).